Elementary Mechanisms of Shear-Coupled Grain Boundary Migration

A. Rajabzadeh,[1,2] F. Mompiou,[1,2] M. Legros,[1,2] and N. Combe[1,2,*]

[1]*Centre d'Elaboration de Matériaux et d'Etudes Structurales, CNRS UPR 8011, 29 rue Jeanne Marvig, BP 94347, 31055 Toulouse cedex 4, France*

[2]*Université de Toulouse, UPS, F-31055 Toulouse, France*

(Received 6 May 2013; published 28 June 2013)

A detailed theoretical study of the elementary mechanisms occurring during the shear-coupled grain boundary (GB) migration at low temperature is performed focusing on both the energetic and structural characteristics. The migration of a $\Sigma 13(320)$ GB in a copper bicrystal in response to external shear displacements is simulated using a semiempirical potential. The minimum energy path of the shear-coupled GB migration is computed using the nudge elastic band method. The GB migration occurs through the nucleation and motion of GB steps identified as disconnections. Energy barriers for the GB and disconnection migrations are evaluated.

DOI: 10.1103/PhysRevLett.110.265507 PACS numbers: 61.72.Mm, 61.72.Ff, 62.20.fq

Nanocrystalline materials (grains sizes <100 nm) present enhanced mechanical properties compared to conventional materials. While the role of dislocations may explain the mechanical properties' enhancements due to grain refinement in the microcrystalline regime (Hall-Petch effect) [1], stress-induced grain boundary (GB) migrations are suggested to be an efficient plasticity mechanism in nanocrystalline metals [2–4].

Among the possible GB-based mechanisms [5], at low temperature, for low- and high-angle GBs, the shear-coupled GB migration has been evidenced as a dominant one both experimentally [2,6,7] and using molecular dynamics simulations [8–10]: the normal GB displacement over a distance m is accompanied by a relative in-plane translation Δd. The coupling factor $\beta = \Delta d/m$ characterizes this mechanism. Numerous theoretical studies have focused on the relation between the coupling factor and the GB geometry [8,11] or on the stick-slip GB migration under a constant shear velocity [12]. Besides, experimental efforts have mainly consisted in measuring the coupling factor [7,11,13].

The present theoretical study addresses the elementary mechanisms occurring during the shear-coupled GB migration at low temperature. Using atomistic simulations based on the nudge elastic band (NEB) method, the shear-coupled GB migration is shown to occur through the nucleation and motion of GB steps, identified as disconnections [14]. Structural and energetic characteristics of these elementary mechanisms are described. The GB migration, generally considered a simple activated process of the stick-slip motion is evidenced as a succession of elementary activated processes in agreement with numerical observations of disconnections [8,15].

The migration of a symmetric tilt GB in response to an external shear deformation is investigated in a copper bicrystal using the molecular dynamics (MD) simulation package LAMMPS [16]. Figure 1(a) shows a sketch of the system under study. The simulation cell contains two symmetric grains of a perfect fcc copper crystal disorientated relatively to each other by an angle $\theta = 67.38°$ around the [001] direction: a symmetric coincident site lattice (CSL) tilt boundary, $\Sigma 13$ (320), results at the interface. The equilibrium configuration of this GB and its shear-coupled migration characteristic have already been studied [12]. Periodic boundary conditions are applied in the $[2\bar{3}0]$ (y-axis) and [001] (z-axis) directions. The cell x size (x axis along the [320] direction) is 10.3 nm. In the following, $L_{[2\bar{3}0]}(L_{[001]})$ refers to the coincident site lattice periodicity along the $[2\bar{3}0]([001])$ direction. The interactions between copper atoms are modeled using an embedded-atom potential [17]. Two 1.5 nm thick slabs at the top and bottom of the cell contain atoms with relative positions frozen to the perfect lattice ones and are used to impose a shear stress on the GB. The equilibrium structure of the $\Sigma 13$ GB is reported in Fig. 1(b) and shows characteristic structural units [12].

The shear-coupled GB migration is studied at 0 K: the slabs are translated relatively to each other in the y direction by small increments and the potential energy is minimized at each step using a conjugate gradient method. Figures 2(a) and 2(b) report the shear stress (calculated using the virial stress tensor) and the potential energy variation as a function of the relative shear displacement d. These results are given for a simulation cell which the y, z sizes, and atom number are 1.3 nm ($1L_{[2\bar{3}0]}$), 1.4 nm ($4L_{[001]}$), and 1664 atoms. Increasing the shear displacement d from the equilibrium initial configuration $d_0 = 0$ in Fig. 2, the shear stress (potential energy) linearly (quadratically) increases and evidences an elastic regime leaving the GB position unchanged compared to its initial position (black curves). This regime breaks up at $d_c = 0.365$ nm where the shear stress drops as the GB migrates. From this point $d > d_c$, an increase in shear displacement d produces a linear increase (red or dark gray curves) of the shear

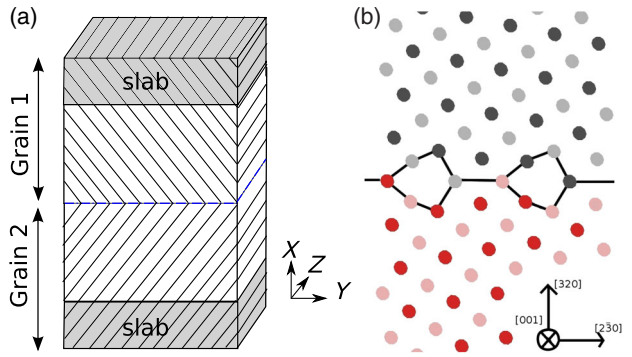

FIG. 1 (color online). (a) Sketch of the simulation cell. (b) Configurations of the $\Sigma 13$ GB projected in the (x, y) plane: Black (gray) and red (pink) atoms belong to different grains. Black (red) and gray (pink) atoms do not have the same z coordinate. For black and white printing, red, gray, and pink atoms appear as dark gray, gray, and light gray atoms.

stress until the next GB migration resulting in a stick-slip behavior [12]. Decreasing the shear displacement d from $d > d_c$ (red or dark gray curves) results in the linear (quadratic) decreases of the shear stress (potential energy): this regime is elastic leaving the GB position unchanged compared to the final GB configuration reached after the first migration. The shear stress cancels and the potential energy is minimum at the equilibrium final GB position

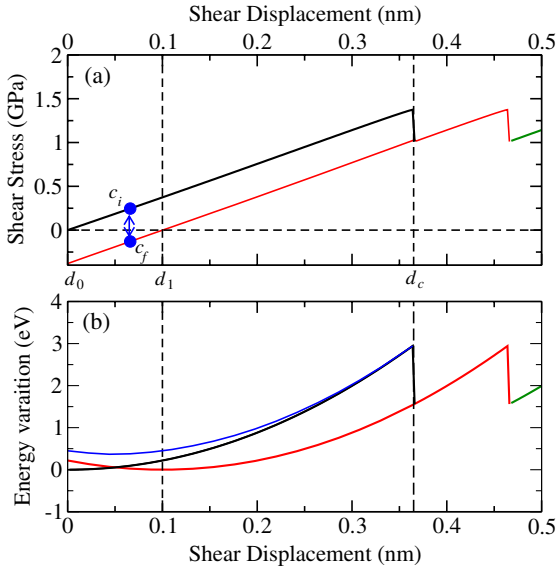

FIG. 2 (color online). (a) Shear stress and (b) potential energy variation (black, red, and green) as a function of the shear displacement. Black and red curves correspond to the initial and final configurations of the GB. The blue curve reports the energy of the transition state from the initial to the final configuration. Dashed lines are a guide to the eyes. c_i and c_f denote the initial RC = 0 and final RC = 1 configurations used in the NEB method with $d = 0.066$ nm [cf Fig. 3(a)]. The cell y and z sizes are 1.3 nm and 1.4 nm. For black and white printing, red and blue curves appear as dark and very dark gray curves.

$d_1 = 0.1$ nm. The normal GB displacement $m = -0.25$ nm (measured from the simulation) is accompanied by a shear displacement $\Delta d = d_1 - d_0$. The coupling factor is $\beta = -0.40$, in agreement with previous studies [12].

While the GB migrates at 0 K for $d = d_c$, at finite temperature, the GB may migrate for $d < d_c$ [12]. To investigate this expected thermally activated migration, configurations of the system before and after the GB migration obtained at 0 K for a given external parameter d are used as initial and final configurations in the climbing image NEB method [18]. The NEB method involving typically 40 images yields the determination of the minimum energy path (MEP) for each value of d. A reaction coordinate (RC), a normalized distance [19] along the energy path, is defined as an indicator of the GB migration progress. Figure 3(a) reports the variation of the potential energy ΔE along the MEP for a shear displacement $d = 0.066$ nm, a representative MEP among those obtained varying d: the NEB is performed between the initial c_i (RC = 0) and final c_f (RC = 1) configurations reported in Fig. 2(a). The MEP presents two local maxima for RC = 0.37 and 0.58 and a metastable state for RC = 0.506. The energy barrier for the GB migration is deduced $\Delta E^{\mathrm{GB}}_{\mathrm{bar}} = 0.283$ eV. Figure 3(b) reports the projection of the initial, metastable and final configurations of the GB in the (x, y) plane. The metastable configuration, a $L_{[001]}$ periodic structure along the z direction, shows a displaced structural unit evidencing two opposite GB steps. Performing a Burgers circuit in the (x, y) plane, the Burgers vectors $\vec{b}_1 = (L_{[2\bar{3}0]}/13)\vec{u}_y$ and $\vec{b}_2 = -\vec{b}_1$ are associated with the left and right steps. Such GB steps,

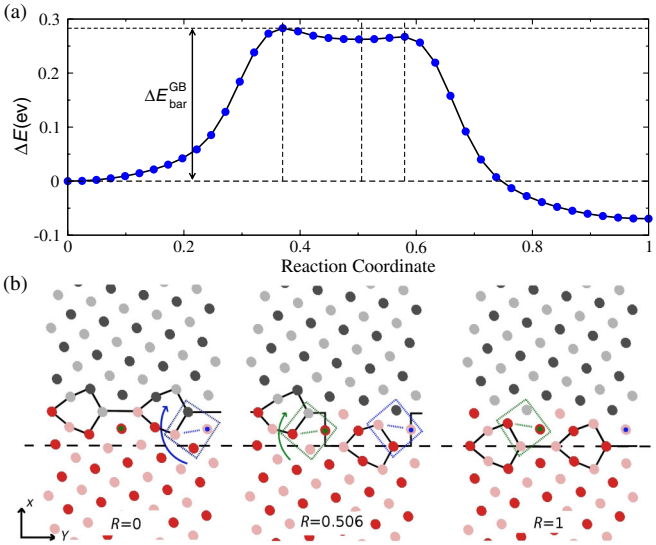

FIG. 3 (color online). (a) MEP energy profile as a function of the RC. (b) Same as Fig. 1(b) for the initial, metastable, and final GB configurations. Black curves are guides to the eyes. Blue and green squares display the main moving atoms. The cell y and z sizes are 1.3 nm and 1.4 nm.

presenting a shear component and a normal displacement (the step height) are, following Ref. [14], disconnections. The ratio between this shear component and the step height is the GB coupling factor. Examining the configurations along the MEP, the appearance and disappearance of the disconnections are mainly induced by the rotation of four atomic columns around the z direction suggesting a shuffling mechanism [20,21]: These columns are enclosed in the blue (right) (RC $= 0 \rightarrow 0.506$) and green (left) squares (RC $= 0.506 \rightarrow 1$) in Fig. 3(b) and the rotation axes nearly coincide with the blue and green points (corresponding to the right corner).

Some additional simulations are performed in cells with y sizes ranging linearly from 1.3 nm ($1L_{[2\bar{3}0]}$) to 6.5 nm ($5L_{[2\bar{3}0]}$) corresponding to 1664 to 8320 atoms (the cell x and z sizes being 10.3 nm and 1.4 nm). Figure 4(a) reports the evolution of the MEP per unit area $\Delta e = \Delta E/A$ (with A the GB area) during the GB migration as a function of the RC for different cell y sizes and for a shear displacement $d = 0.066$ nm. The MEP per unit area presents an increasing number of local extrema with the simulation cell y size. The structural analysis shows that the GB migration occurs through the formation and motion in opposite directions of two (opposite) disconnections per cell regardless the cell y size. As an example, in the larger cell (6.5 nm y size) containing ten structural units, the configurations where the structural units have been successively displaced

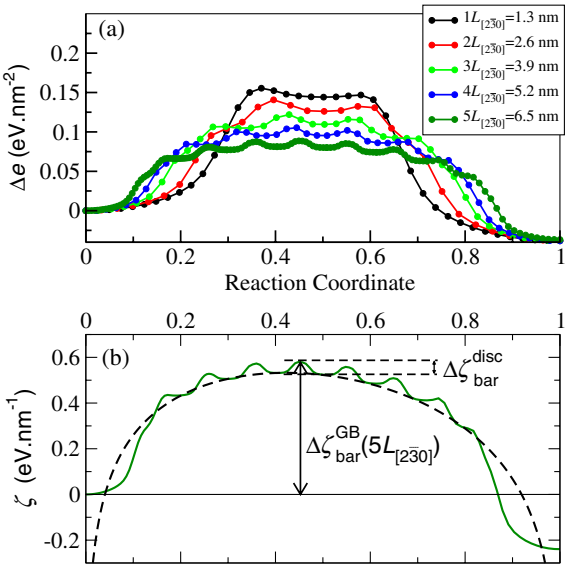

FIG. 4 (color online). (a) Minimum energy path per unit area as a function of the RC for $d = 0.066$ nm for 5 different cell y sizes ranging from 1 to $5L_{[2\bar{3}0]}$ (z size is 1.4 nm). (b) Minimum energy path (solid line) per unit disconnection length as a function of the RC for $d = 0.066$ nm (the cell y and z size are 6.5 nm and 1.4 nm) and energy variation (dashed line) for stable configurations, as fitted from elasticity theory Eq. (1). The quantities $\Delta\zeta^{GB}_{bar}$ and $\Delta\zeta^{disc}_{bar}$ are roughly reported.

correspond either to a minimum or a shoulder (at RC $=$ 0.13, 0.79, and 0.84) in the MEP.

Below, the disconnection formation is shown to be the limiting step of the migration. To this aim, the MEP curves are interpreted within the elasticity theory. In the following, all quantities denoted by ζ refer to energies per disconnection unit length. The excess energy ζ due to the presence of two opposite parallel disconnections separated by a distance a reads [22]:

$$\zeta(a) = 2\zeta_{\text{form}}(r_c) + \zeta_{\text{inter}}(a, r_c) + \zeta_{\text{stress}}(a), \qquad (1)$$

$\zeta_{\text{form}}(r_c)$ is the disconnection formation energy (r_c the core radius). $\zeta_{\text{inter}}(a, r_c)$ is the elastic interaction energy between the disconnections and their images (periodic boundary conditions in the y direction): if the disconnection cores do not overlap, analytical calculations using the linear isotropic theory of elasticity (with Poisson's ratio ν and shear modulus μ) yield: $\zeta_{\text{inter}}(a, r_c) = (\mu b_1^2/2\pi(1-\nu))\ln[(L_y/\pi r_c)\sin(\pi a/L_y)]$. $\zeta_{\text{stress}}(a)$ is the work of internal forces during the disconnection motion in the absence of disconnection interactions, i.e., the energy change produced by the displacement a of a single disconnection in an infinite GB interface: $\zeta_{\text{stress}} = (e_{\text{final}} - e_{\text{initial}})a$ with e_{final} (e_{initial}) the energy per unit area of a system with a plane GB in its final (initial) position. $e_{\text{final}} - e_{\text{initial}}$ deduces from Fig. 2(b). Examining the metastable configurations along the MEP, the disconnection distance a is found to linearly vary with RC: $a = L_y$ RC. Figure 4(b) reports the excess energy ζ derived from the NEB calculations (solid curve) in the larger cell (6.5 nm y size) and the fit (dashed curve) of the metastable configurations curve by the expression: $\zeta(a) = 2\zeta_{\text{form}}(r_c) + K\ln[(L_y/\pi r_c)\sin(\pi a/L_y)] + (e_{\text{final}} - e_{\text{initial}})a$. Values of $\zeta_{\text{form}}(r_c) = 0.053$ eV $\cdot$ nm^{-1} (using r_c the copper lattice parameter 0.3615 nm) [23] and $K = 0.3059$ eV $\cdot$ nm^{-1} are deduced. Though the expression $\zeta_{\text{inter}}(a, r_c)$ is established using the isotropic linear elasticity, its application to the present case is satisfactory [24]. From the subtraction of the MEP with Eq. (1), the disconnection motion energy barrier is deduced $\Delta\zeta^{\text{disc}}_{\text{bar}} \approx 52 \pm 4$ meV$\cdot$nm^{-1}. The energy barrier $\Delta\zeta^{\text{disc}}_{\text{bar}}$ for a disconnection motion is about 11 times smaller than the energy barrier $\Delta\zeta^{\text{GB}}_{\text{bar}}(5L_{[2\bar{3}0]}) = 578$ meV$\cdot$nm^{-1} [measured from Fig. 4(b)] for the GB migration in the larger cell in qualitative agreement with recent simulation results [25]. Though rigorously dependent on the disconnection formation and motions, the GB migration rate is essentially controlled by the formation of a critical nucleus composed of two disconnections.

Figure 5 reports the energy barrier for the GB migration per unit disconnection length $\Delta\zeta^{\text{GB}}_{\text{bar}}(L_y)$ as measured and defined from Fig. 4(b) as a function of the shear displacement d in the range $0 < d < d_c$ for different cell y sizes. For a given cell y size, $\Delta\zeta^{\text{GB}}_{\text{bar}}(L_y)$ cancels for $d = d_c$ in agreement with the spontaneous migration of the GB at 0 K. $\Delta\zeta^{\text{GB}}_{\text{bar}}(L_y)$ decreases with d: the work of the external

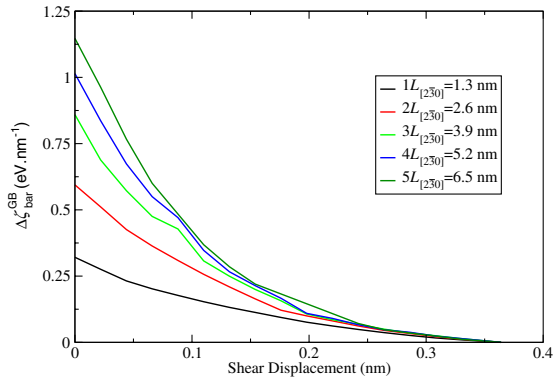

FIG. 5 (color online). Energy barrier per unit disconnection length $\Delta\zeta_{bar}^{GB}$ as a function of the shear displacement for 5 different cell y sizes ranging from 1 to $5L_{[2\bar{3}0]}$ (z size is 1.4 nm).

force applied to the slabs to displace them is positive. This work not only affects the initial and final configuration energies [black and red curves in Fig. 2(b)], but also the transition state energy (blue curve).

In our simulation model, due to the periodic boundary conditions in the y direction, the metastable configurations of the GB migration mechanism correspond to the formation of a regular array (whose period is the cell y size) of opposite disconnections. However on an infinite GB interface, following Eq. (1), the GB migration mechanism presenting the lowest energy barrier per unit GB area corresponds to the formation of a single critical nucleus composed of two disconnections and their further motion on an infinite GB interface. On one hand, the energy barrier per unit disconnection length $\Delta\zeta_{bar}^{GB}(\infty)$ to form such a critical nucleus can be estimated from Eq. (1). In the limit $L_y \to \infty$, ζ is stationary for $a_c = -K/(e_{final} - e_{initial})$. So that the GB migration mechanism presents a critical nucleus only if $a_c > 0$, i.e., $e_{final} - e_{initial} < 0$ or from Fig. 2(b), $d > 0.05$ nm. For $d = 0.066$ nm, $\Delta\zeta_{bar}^{GB}(\infty) = 748$ meV $\cdot$ nm^{-1} is found. On the other hand, $\Delta\zeta_{bar}^{GB}(\infty)$ can also be estimated from values of $\Delta\zeta_{bar}^{GB}(L_y)$ reported in Fig. 5: $\Delta\zeta_{bar}^{GB}(L_y)$ increases with the cell y size and tends to converge with the simulation cell y size at least for large values of d. For small values $d < 0.05$ nm, $\Delta\zeta_{bar}^{GB}(L_y)$ is not expected to converge with the cell y size, from the analysis above. For intermediate values $0.05\,\text{nm} < d \lesssim 0.1$–$0.15\,\text{nm}$, the convergence is not complete as evidenced by the comparison between the energy barrier in the biggest cell $\Delta\zeta_{bar}^{GB}(5L_{[2\bar{3}0]}) = 578$ meV $\cdot$ nm^{-1} and the theoretical estimation $\Delta\zeta_{bar}^{GB}(\infty) = 748$ meV $\cdot$ nm^{-1} for $d = 0.066$ nm.

Finally, the dependence of the energy barrier $\Delta\zeta_{bar}^{disc}$ for the disconnection motion has been found to weakly vary with the shear displacement d. Regarding the incertitude of the measure of $\Delta\zeta_{bar}^{disc}$, the quantitative characterization of this dependence is not possible, so that in first approximation, this energy barrier can be considered as invariant with the shear displacement.

In conclusion, the elementary mechanisms of the shear-coupled GB migration in a copper bicrystal have been evidenced. Complementary to the common stick-slip GB motion presentation, the GB migration occurs through the nucleation and motion of GB disconnections in agreement with recent simulations [15]. The nucleation is the rate limiting process. These elementary mechanisms are supported by recent experimental results evidencing the formation of GB macrosteps [7]. Such a migration mechanism limited by the disconnections nucleation applies if the temperatures or GB areas (in nanocrystalline metals) are small enough to prevent numerous quasisimultaneous nucleation on the same GB interface.

The present study opens numerous perspectives to the investigation of the elementary processes of low temperature GB migration. First, extending the simulation cell in the z direction, the elementary mechanism of the formation and migration of disconnections can be investigated: some preliminary calculations, show that these processes are not invariant by translation along z, evidencing some disconnection kinks. A forthcoming publication will be devoted to this study. Second, the present study, and more precisely the developed method [26] is easily transposable to the investigation of any GB. In addition, since several MD studies [8,12,15] have reported the observation of GB steps, we are confident that the shear-coupled GB migration mechanism involving the nucleation and motion of disconnections is not specific to the $\Sigma 13(320)$ GB of copper but can be applied to numerous GBs including the low-, high-angle, and asymmetrical GB in various materials.

This work was performed using HPC resources from CALMIP (Grant No. 2012-12172). Authors acknowledge M. Benoit, D. Caillard, J. Morillo, H. Tang, and N. Tarrat for fruitful discussions.

*nicolas.combe@cemes.fr

[1] E. Hall, Proc. Phys. Soc. London Sect. B **64**, 747 (1951); N. J. Petch, J. Iron Steel Inst. **174**, 25 (1953).
[2] M. Legros, D. Gianola, and K. Hemker, Acta Mater. **56**, 3380 (2008).
[3] M. Jin, A. M. Minor, E. A. Stach, and J. W. Morris, Acta Mater. **52**, 5381 (2004).
[4] J. Schäfer and K. Albe, Acta Mater. **60**, 6076 (2012).
[5] M. A. Meyers, A. Mishra, and D. J. Benson, Prog. Mater. Sci. **51**, 427 (2006).
[6] K. Zhang, J. R. Weertman, and J. A. Eastman, Appl. Phys. Lett. **87**, 061921 (2005).
[7] A. Rajabzadeh, M. Legros, N. Combe, F. Mompiou, and D. A. Molodov, Philos. Mag. **93**, 1299 (2013).
[8] J. W. Cahn, Y. Mishin, and A. Suzuki, Acta Mater. **54**, 4953 (2006).
[9] M. Velasco, H. V. Swygenhoven, and C. Brandl, Scr. Mater. **65**, 151 (2011).
[10] E. R. Homer, S. M. Foiles, E. A. Holm, and D. L. Olmsted, Acta Mater. **61**, 1048 (2013).

[11] F. Mompiou, D. Caillard, and M. Legros, Acta Mater. **57**, 2198 (2009); D. Caillard, F. Mompiou, and M. Legros, Acta Mater. **57**, 2390 (2009).
[12] Y. Mishin, A. Suzuki, B. Uberuaga, and A. Voter, Phys. Rev. B **75**, 224101 (2007).
[13] T. Gorkaya, D. A. Molodov, and G. Gottstein, Acta Mater. **57**, 5396 (2009).
[14] J. Hirth and R. Pond, Acta Mater. **44**, 4749 (1996).
[15] L. Wan and S. Wang, Phys. Rev. B **82**, 214112 (2010).
[16] S. J. Plimpton, J. Comp. Physiol. **117**, 1 (1995).
[17] Y. Mishin, M. Mehl, D. Papaconstantopoulos, A. Voter, and J. Kress, Phys. Rev. B **63**, 224106 (2001).
[18] G. Henkelman, B. P. Uberuaga, and H. Jonsson, J. Chem. Phys. **113**, 9901 (2000).
[19] It is the cumulative distance (normalized by the total cumulative distance) between adjacent replicas in the configuration space (dimension $3N$, N the number of atoms).
[20] S. Babcock and R. Balluffi, Acta Metall. **37**, 2367 (1989).
[21] F. Mompiou, M. Legros, and D. Caillard, Acta Mater. **58**, 3676 (2010).
[22] J. P. Hirth and J. Lothe, *Theory of Dislocations* (Krieger Publishing Company, Malabar, 1992).
[23] R. J. Kurtz, R. G. Hoagland, and J. P. Hirth, Philos. Mag. A **79**, 683 (1999).
[24] Note that we have also checked that the prefactor K weakly depends on the size L_x of the cell.
[25] H. Khater, A. Serra, R. C. Pond, and J. P. Hirth, Acta Mater. **60**, 2007 (2012).
[26] A stress load at 0 K to induce the GB migration, a stress unload to generate the final configuration and finally, the NEB study between the initial and final configuration.